



## ELECTRIC FIELD STRESS ANALYSIS OF DIFFERENT SPACERS IN GIS

Sonali S. Kulkarni<sup>1</sup>, P.C.Tapre<sup>2</sup>, C.Veeresh<sup>3</sup>, Krutika T.Agrawal<sup>4</sup>

<sup>1,2,3,4</sup>Electrical, SND College of Engineering,(India)

### ABSTRACT

Gas Insulated systems (GIS) require solid insulating materials to provide mechanical support for conductors as well as to separate two compartments. Hence there is a need for control of electric field stresses at spacer surface in order to reduce internal discharges also surface discharges to the enclosure surface. As several failures in GIS system have been reported in many installations around the world. A high percentage of these failures are due to improper design of the spacers shape or manufacturing defects. The breakdown of SF6 gas insulation is adversely affected by the presence of spacer especially at the interface point formed by solid insulating spacer and SF6 gas. This point represents the weakest point at the GIS and hence there is a need for control of electric stresses at spacer surface. In order to reduce such distortion the spacers used in the gas insulated systems designed to realize more or less uniform field distribution along their surfaces. In this research a comprehensive study of the factors affecting the electric field distribution on the spacer's surface has been carried out. So three spacer's shapes have been considered. The finite element method (FEM) has been used throughout the calculation, as this method has proved to be more accurate than other methods.

**Keywords:** *Spacer's Shapes, Composite Cone Spacer, Triple Junction Point, Finite Element Method (FEM)*

### I. INTRODUCTION

The breakdown of SF6 gas insulation is adversely affected by the presence of insulator surfaces, unless special design precautions are taken. Gas Insulated systems require solid insulating materials to provide mechanical support for conductors. For the enhancement of insulation reliability and compact design in gas insulated power equipment the solid insulators play crucial role of electrical insulation [1]. The study of electric field distribution in and around the supporting spacers has been of considerable interest for the design engineer for designing the equipment operating at high voltage levels [2, 3]. The presence of spacers, results in complex-dielectric field distribution. It often intensifies the electric field particularly on the spacer's surface. The insulation ability of SF6 is highly sensitive to the maximum electric field, and furthermore the insulation strength along a spacer's surface is usually lower than that in the gas space [4]. So the spacers used in GIS should be precisely designed to realize more or less uniform field distribution along their surfaces. Effort is to be made to decrease the electric field value as low as possible keeping in mind the optimum leakage path. Spacer's profile is considered the main variable, which controls the field distribution and hence field uniformity can be achieved by adopting the appropriate profile [5,6]. Consider, for example, a horizontal coaxial conductor arrangement. A particle



lying on the inner surface of the outer conductor will obtain a charge, which is proportional to the local field. Thus, the particle experiences an electrostatic force. At sufficiently high applied voltage, the particle will lift off and begin to move in the gas space between the conductors. At a sufficiently HV, a particle is able to cross the gap between the conductors and can initiate breakdown. Experimental and theoretical studies have shown that particle initiated breakdown is a two-stage process [4,5].

## II. CONCEPT OF FEM

### 2.1 Finite Element Method (FEM)

FEM is a suite of programs for solving low frequency electromagnetic problems on two- dimensional planar and axisymmetric domains. The program currently addresses linear/nonlinear magnetostatic problems, linear/nonlinear time harmonic magnetic problems, linear electrostatic problems, and steady-state heat flow problems.

FEMM is divided into three parts:

- Interactive shell
- Triangle
- Solvers

#### 2.1.1 Interactive shell

This program is a Multiple Document Interface pre-processor and a post-processor for the various types of problems solved by FEMM. It contains a CAD like interface for laying out the geometry of the problem to be solved and for defining material properties and boundary conditions. AutoCAD DXF files can be imported to facilitate the analysis of existing geometries. Field solutions can be displayed in the form of contour and density plots. The program also allows the user to inspect the field at arbitrary points, as well as evaluate a number of different integrals and plot various quantities of interest along user-defined contours.

#### 2.1.2 Triangle

Triangle breaks down the solution region into a large number of triangles, a vital part of the finite element process.

#### 2.1.3 Solvers

Each solver takes a set of data files that describe problem and solves the relevant partial differential equations to obtain values for the desired field throughout the solution domain.

## 2.2 Relevant Partial Differential Equations

Electrostatic problems consider the behavior of electric field intensity,  $E$ , and electric flux density (alternatively electric displacement),  $D$ . There are two conditions that these quantities must obey. The first condition is the differential form of Gauss' Law, which says that the flux out of any closed volume is equal to the charge contained within the volume:

$$\Delta \cdot D = \rho \quad (2.1)$$

where  $\rho$  represents charge density. The second is the differential form of Ampere's loop law:



$$\Delta \times E = 0 \quad (2.2)$$

Displacement and field intensity are also related to one another via the constitutive relationship:

$$D = \epsilon E \quad (2.3)$$

Where,  $\epsilon$  is the electrical permittivity. Although some electrostatics problems might have a nonlinear constitutive relationship between  $D$  and  $E$ , the program only considers linear problems. To simplify the computation of fields which satisfy these conditions, the program employs the electric scalar potential,  $V$ , defined by its relation to  $E$  as:

$$E = -\Delta V \quad (2.4)$$

Because of the vector identity  $\Delta \times \Delta \psi = 0$  for any scalar  $\psi$ , Ampere's loop law is automatically satisfied. Substituting into Gauss' Law and applying the constitutive relationship yields the second order partial differential equation:

$$-\epsilon \Delta^2 V = \rho \quad (2.5)$$

which applies over regions of homogeneous  $\epsilon$ . The program solves (2.5) for voltage  $V$  over a user-defined domain with user-defined sources and boundary conditions.

## 2.3 Finite Element Analysis

Although the differential equations of interest appear relatively compact, it is typically very difficult to get closed-form solutions for all but the simplest geometries. This is where finite element analysis comes in. The idea of finite elements is to break the problem down into large number regions, each with a simple geometry (e.g. triangles). For example, Figure 4.1 shows a random semicircle broken down into triangles. Over these simple regions, the "true" solution for the desired potential is approximated by a very simple function. If enough small regions are used, the approximate potential closely matches the exact solution. The advantage of breaking the domain down into a number of small elements is that the problem becomes transformed from a small but difficult to solve problem into a big but relatively easy to solve problem. Through the process of discretization, a linear algebra problem is formed with perhaps tens of thousands of unknowns. However, algorithms exist that allow the resulting linear algebra problem to be solved, usually in a short amount of time. Specifically, FEMM discretizes the problem domain using triangular elements. Over each element, the solution is approximated by a linear interpolation of the values of potential at the three vertices of the triangle. The linear algebra problem is formed by minimizing a measure of the error between the exact differential equation and the approximate differential equation as written in terms of the linear trial functions.

## III. THE ELECTRIC FIELD CALCULATION AND DISCUSSION FOR DIFFERENT SPACER'S SHAPES

There are different types shapes of spacer which used in GIS, these spacers fundamentally are divided into two types according to their shapes, namely; the disc and cone type. Spacer's shapes in a coaxial GIS shown in fig.(1), Which have symmetry about the Z-axis, the system arrangements are characterized by six dimensional variables, ( $r_o$ ,  $R$ ,  $Z_s$ ,  $Z_e$ ,  $S$ ,  $\theta$ ). Where  $r_o$ ,  $R$  are the radius of the inner and outer electrodes respectively,  $Z_s$  and  $Z_e$  are the spacers half thickness at the inner and outer electrodes arrangements respectively as indicated in Fig.

(1-a), also (S) and ( $\theta$ ) are the thickness and the inclination angle of the cone spacer as shown in Fig. (1- b). the obtained results in this research are expressed by the normalized values. Where  $r_0$  is the based dimensional value which equal to 10 cm and the applied voltage is the base voltage value which equal to 100kv.

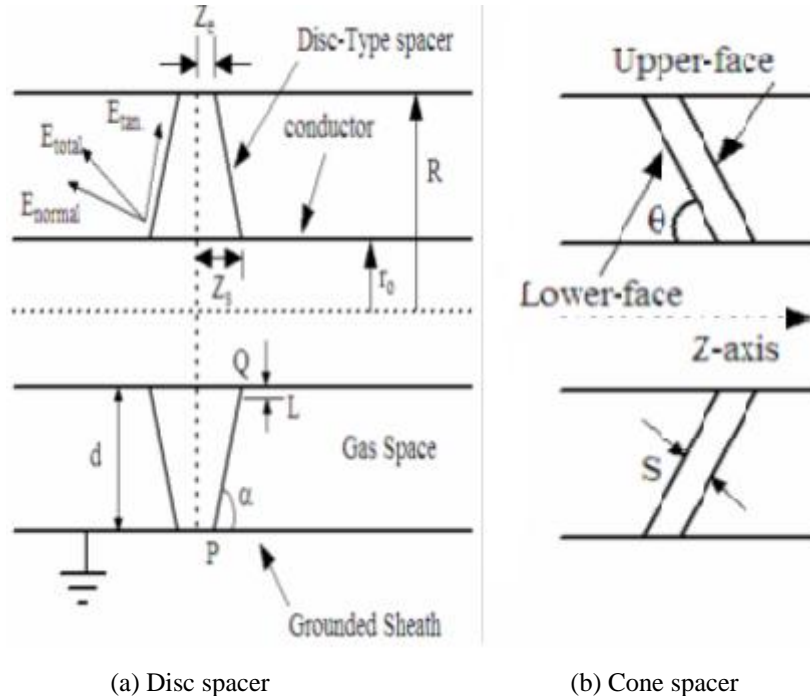


**Fig.(1)Spacer electrode arrangements in GIS**

### 3.1 Electric Field Calculations around Disc Spacer

For the spacer’s shape indicated in figure (1-a).The effects of its dimensions and its relative permittivity are carried out.

#### 3.1.1 Effect of the Spacer’s Dimensions on the Electric Field Distribution

Figure (2) shows the electric field distribution for disc spacer with different dimensions. The results are obtained by fixing  $Z_e$  , R and permittivity ( $\epsilon_r$ ) values at 0.2,3 P.U and 6 respectively. The only variable is  $Z_s$  with values between 0.2 to 2p.u.

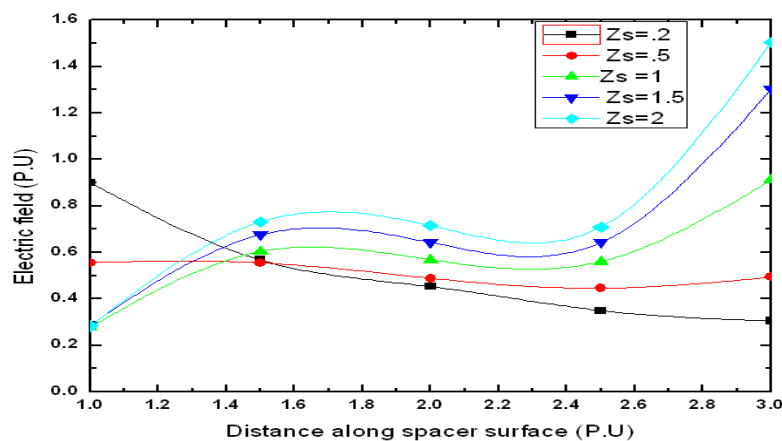


**Fig. (2) Effect of  $Z_s$  on the electric field distribution along the spacer surface**

From fig.(2) It can be observed that, the electric field distribution at  $Z_s=0.2p.u$  is uniform as ( $\alpha =90$ ), for spacer has  $Z_s<0.2p.u$ , the electric field decreases around the inner electrode and increases around the outer electrode .Also it can be observed that, the electric field near the triple junction especially at outer electrode increases as  $Z_s$  increases .So from these figures it can be concluded that the spacer dimensions effect on the electric field distribution on and around the spacer surface. This result is identical for result [10].

### 3.1.2 Effect of the spacer relative permittivity on the Electric Field Distribution for Disc Spacer

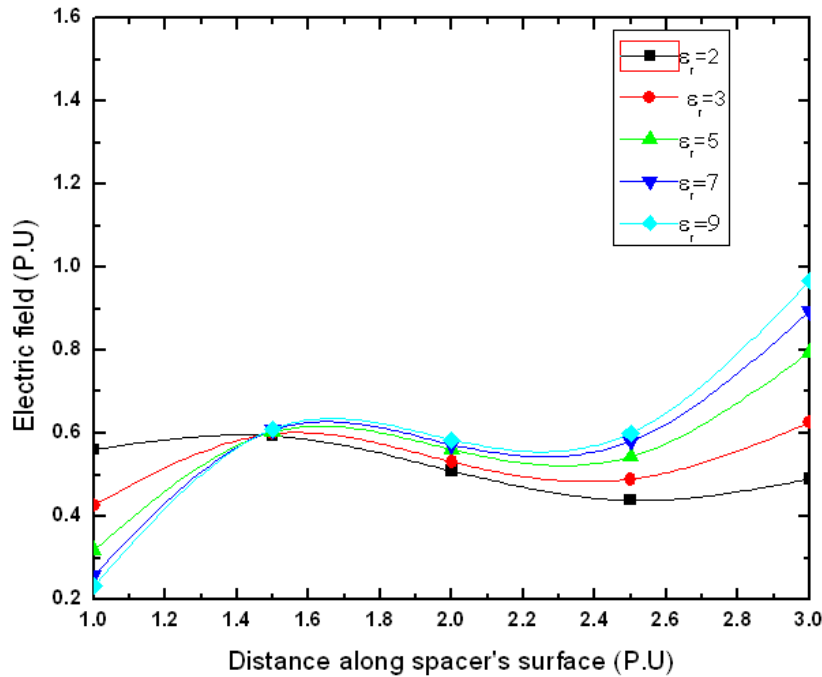


Fig. (3) Effect of spacer’s relative permittivity on the electric field distribution along surface of disc spacer

The results of Fig. (3) Shows the electric field distribution for disc spacer with different permittivity values were obtained for fixed values of  $Z_s$ ,  $Z_e$  and  $R$  at 1, 0.2 and 3p.u respectively. The only variable is the spacer relative permittivity which varies between 2 and 9.From this figure it is observed that the spacer permittivity effect on the electric field distribution.

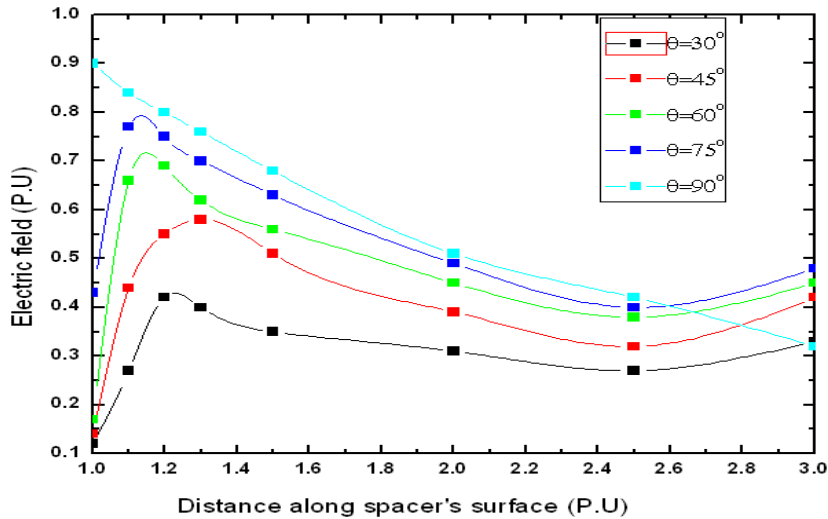
### 3.2 Electric Field Calculations around Cone spacer

The effect of spacer’s inclination angle ( $\theta$ ) and spacer’s thickness ( $S$ ) for cone spacer on the electric field distribution along its surface can be studied as shown in figure (2-b).

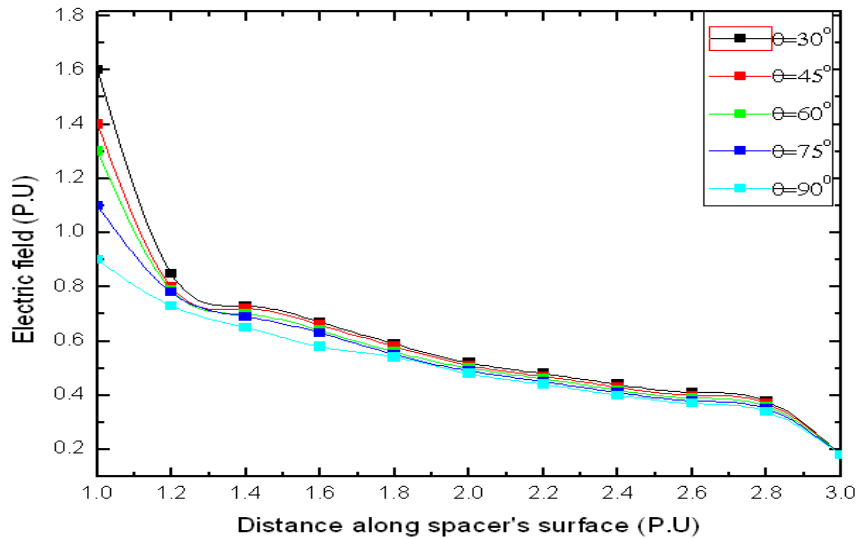
#### 3.2.1 Effect of the spacer’s inclination angle on the electric field distribution

Figure (4) shows the effect of changing of the spacers inclination angle ( $\theta$ ) on the total electric field distribution on its upper surface, that obtained at fixed values of  $S, R$ , and  $\epsilon_r$  constant at 0.2,3p.u and 6 respectively . From this figure it can be shown that the electric field is higher near the inner electrode and then it reduces gradually towards the outer electrode, also it is clear that the electric field decreases with the decreasing of ( $\theta$ ).However;

there is no noticeable effect of ( $\theta$ ) on the total electric field distribution on the lower surface except near to the inner electrode as shown in figure (5).



**Fig. (4) Effect of inclination angle on the electric field distribution along upper cone surface**



**Fig.(5)Effect of inclination angle on the electric field distribution along the lower cone surface**

### 3.2.2 Effect of spacer's thickness on The Electric Field Distribution

Figures (6) and (7) show the effect of changing spacer's thickness ( $S$ ) on the total electric field distribution on its upper and lower surface respectively. This results were obtained at fixed values of  $R$ ,  $\theta$  and  $\epsilon_r$  at  $3p.u, 50\epsilon_0$  and  $6$  respectively and the only variable is the spacer's thickness which has these values  $0.1, 0.2$  and  $0.4p.u$ . From figure (6), we notice that the maximum value of the electric field decreases with the increasing of the spacer's thickness, and the maximum field value shifted towards the outer enclosure. However, there is no observed effect of ( $S$ ) on the total electric field distribution on the lower spacer's surface except near the inner electrode as shown in figure (7).

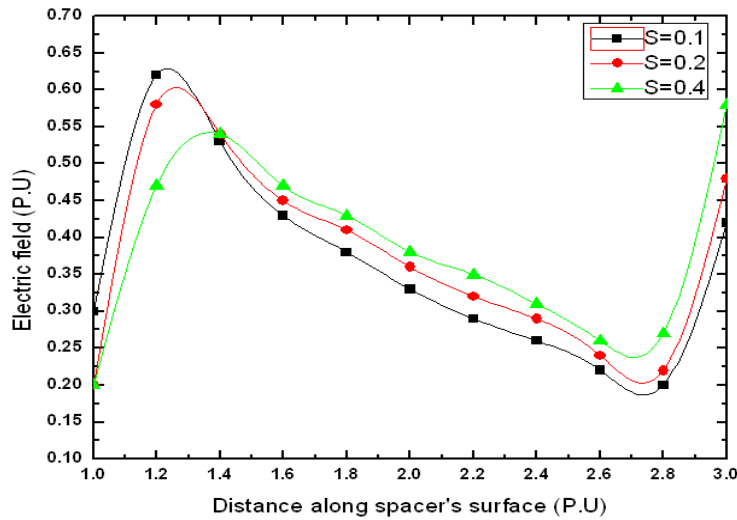


Fig. (6) Effect of spacer's thickness on the electric field distribution along its upper surface

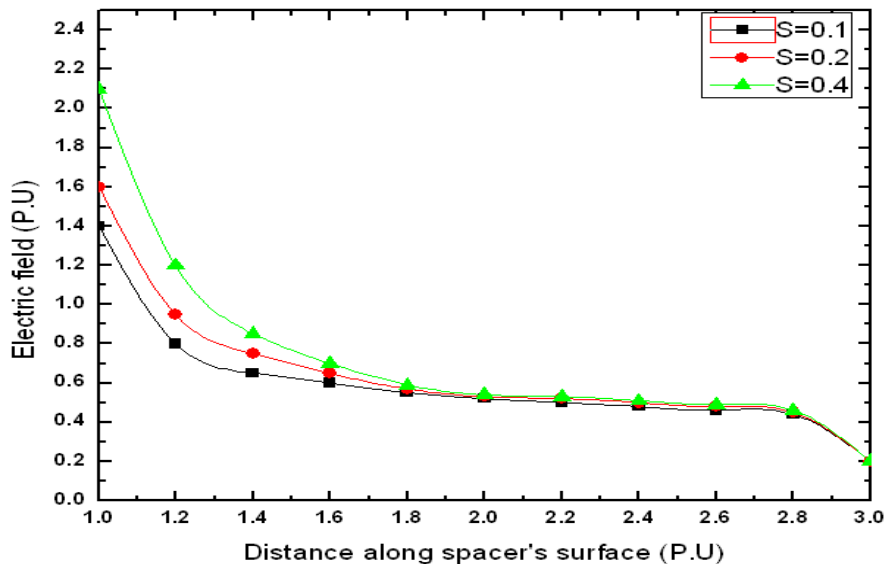


Fig. (7) Effect of spacer's thickness on the electric field distribution along its lower surface

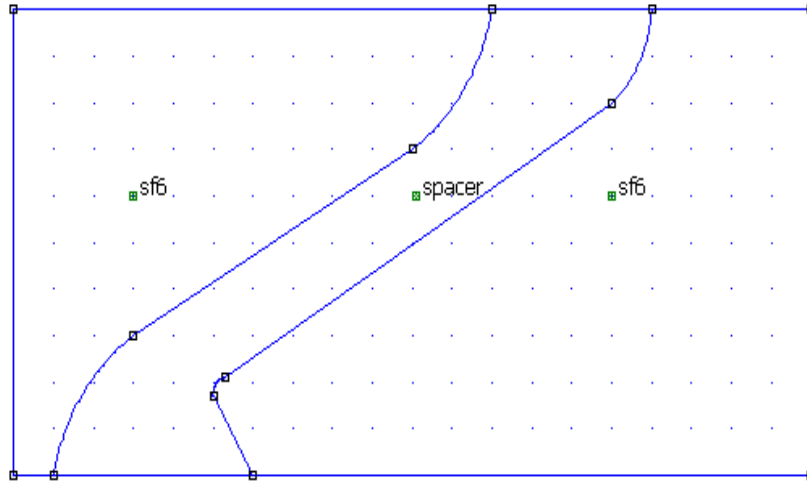
### 3.3 Composite Cone Type Spacer

A composite cone shaped spacer was modeled which combines the advantage of the long leakage distance of a cone shaped profile with that of the quasi-uniform field distribution of a disc-shaped profile [8].

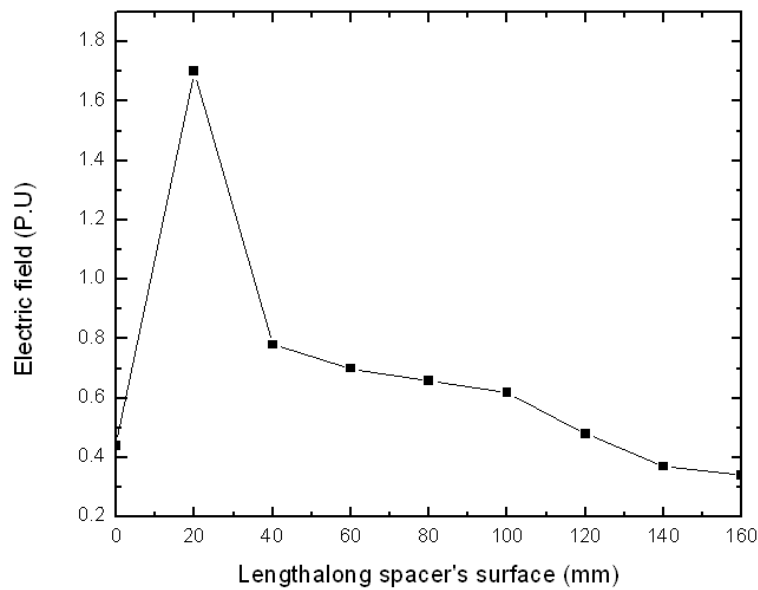
#### 3.3.1 Initial composite cone spacer shape

Figure (8) show the composite cone spacer with these dimensions,  $r_o$  is the outer enclosure radius,  $r_i$  is the inner conductor radius, the difference between  $r_o$  and  $r_i$  is equal to 100mm and its  $\epsilon_r$  equal 6 . This spacer has two sides convex and concave side. It was assumed that no surface charge is accumulated on these sides of spacer. A 1Volt is applied to anode while the cathode is maintained at grounded potential. It can be observed from figure

(9) that the electric field is intensified at the sharp edges ( $r$ ); these values of the electric field may lead to flash over.



**Fig. (8) Initial composite cone spacer shape**



**Fig. (9) Electric field distribution along concave side of initial shape at  $r=4\text{mm}$**

### 3.3.2 Optimized spacer profile

It can be observed from figure (9) that the electric field is intensified at the sharp edges ( $r$ ); these values of the electric field may lead to flash over. So spacer shape control is done by modifying in the sharp edge ( $r$ ) to obtain uniform Electric field distribution along the spacer surface, the only variable in the spacer shape is the sharp edge ( $r$ ) so there are different cases at different ( $r$ ) values as shown in figure (10) where the optimized spacer profile at  $r=28\text{ mm}$ [8].



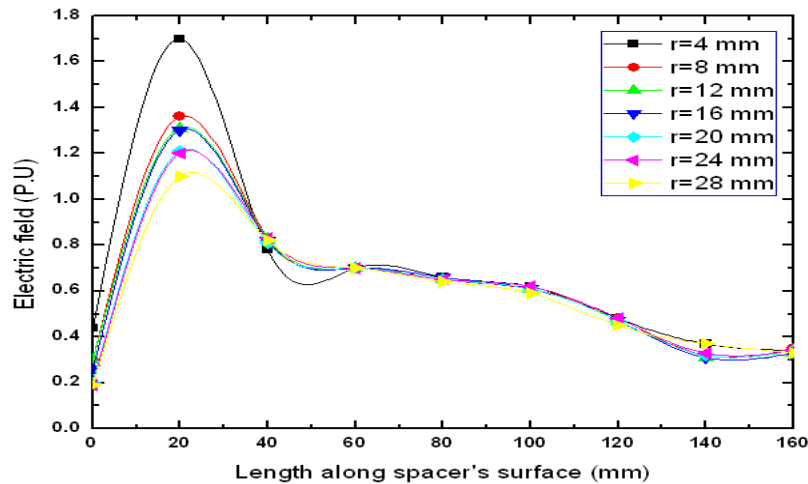


Fig. (10) Electric field distribution along concave spacer surface at different values of (r)

## IV. CONCLUSION

Precise simulation and geometric optimization of the electric field distribution on dielectrics is a key aspect in the design and optimization process of high voltage apparatus. As from results it can be included that, the geometrical shape of the spacer has a significant influence on the electric field distribution. The spacer's material type affect on the electric field distribution on and around the spacer surface. Then a composite cone type spacer is designed geometrically to obtain uniform electric field along the concave side of spacer.

## REFERENCES

- [1] T.Nitta, Y.Fujiwara, F.Endo, J.Ozawa, "Effects of electrode and solid insulator on the flashover in compressed SF<sub>6</sub>, CIGRE Report No. 15-04, 1976.
- [2] Haddad and D.Warne, "Advances in High Voltage Engineering", The Institution of Electrical Engineers, pp. 37- 76,2004.
- [3] J.Sato, T.Shioiri, M.Miyazawa, T.Yoshida and K.Yokokura, "Composite Insulation Technology for New Compact 72/84kV CGIS", IEEE *Transaction on Dielectrics and Electrical Insulation*, Vol.2, pp.489-494, 1999.
- [4] F. Messerer and W. Boeck, "Field Optimization of An HVDC-GIS Spacer", Annual Report, IEEE Conference of Electric Insulation and Dielectric Phenomena (CEIDP), Atlanta, pp.15-18, 1998.
- [5] T. Takuma and T. Watanabe, "Optimal Profiles of Disc-Type Spacer For Gas Insulation", *Ploc. IEE*, Vol. 122. No.2, pp. 183-188, February 1975.
- [6] D. Deepak Chowdary and J.Amarnath, "Electric Field Stress Analysis For A Composite Cone Type Spacer Designed For Uniform Electric Field Distribution On Spacer Surface In The Presence Of A Wire Like Particle", *International Journal of Advances in Engineering & Technology*, Vol. 3, Issue 2, pp. 243-252, May 2012.